

Learning Human-Inspired Force Strategies for Robotic Assembly

Stefan Scherzinger¹, Arne Roennau¹ and Rüdiger Dillmann¹

Abstract—The programming of robotic assembly tasks is a key component in manufacturing and automation. Force-sensitive assembly, however, often requires reactive strategies to handle slight changes in positioning and unforeseen part jamming. Learning such strategies from human performance is a promising approach, but faces two common challenges: the handling of low part clearances which is difficult to capture from demonstrations and learning intuitive strategies offline without access to the real hardware. We address these two challenges by learning probabilistic force strategies from data that are easily acquired offline in a robot-less simulation from human demonstrations with a joystick. We combine a Long Short-Term Memory (LSTM) and a Mixture Density Network (MDN) to model human-inspired behavior in such a way that the learned strategies transfer easily onto real hardware. The experiments show a UR10e robot that completes a plastic assembly with clearances of less than 100 micrometers whose strategies were solely demonstrated in simulation.

I. INTRODUCTION

Many industrial assembly processes require mounting together individual components to build complex products. When plug-inserting two individual parts, this is referred to as the peg-in-hole problem and is often used to benchmark new methods in robotics research. In industry, offline programming [1] is an established process of deriving robot programs before fine-tuning and deploying them on a plant. This process of *fine motion planning* [2] is particularly challenging for force-sensitive assembly: Stiff contacts and rigid fixtures can build up high reaction forces between the robot and the environment, and usually require careful calibration of the robots' motion to process parameters such as friction. On-site, expert knowledge is often needed due to the complexity of the programming.

In general, the inclusion of force-torque sensor signals seems crucial for assembly success [3], [4], [5] and is still used today in form of analytical solutions [6], [7]. Advances in lightweight robots enable a task-optimized impedance design and achieve robust assembly skills that are comparable to human performance [8], [9]. Using the force-torque signals for control policies can also be learned by the robots from trial-and-error [10], which has been shown for insertion tasks with tight clearances [11], [12]. On the contrary, humans are particularly good at handling these tasks manually by using sophisticated senses with a high bandwidth of information. Although being intuitive for us where to press, turn and jolt to get two parts mated when using our hands, these strategies are fuzzy and difficult to describe quantitatively for robot programs. Capturing and translating these skills into suitable

algorithms is an exciting challenge. In this paper, we consider offline programming for assembly, where motion is highly constrained and the parts have low clearances and tight fits. The principle idea is to find technical representations for these human-inspired skills that can be transferred to real hardware once programmed.

To work toward this goal, we propose *probabilistic force strategies*, a data-driven approach to mimic human behavior for low-clearance assembly skills that we build onto force control on industrial manipulators. Our proposed deep neural networks learn from data that is obtained easily offline through showing the task in simulation on simplified primitives with a joystick. Building on the experience from our earlier approach [13], we redesign the previous neural network architecture and present a new concept for modeling the quintessence of human behavior especially for low-clearance assembly.

II. PROBLEM STATEMENT AND RELATED WORK

The peg-in-hole problem is well-known in the assembly literature. Shapes and sizes vary but the parts usually share a single insertion direction. In addition to low tolerances and tight fits, we extend this to various insertion directions with higher geometric complexity in contact. Low-clearance assembly means dealing with force closure and form closure adaptively during execution, caused by inevitable model inaccuracies. The additional challenge in offline programming, however, is programming these skills without real hardware.

We follow the core idea to learn these skills from human demonstrations, which is known under Programming by Demonstration (PbD) [14], [15], Imitation Learning (IL) [16] in physiological neurosciences, and Behavioral Cloning (BC) [17] from machine learning in general. The following sections discuss related works.

A. Probabilistic skill learning from demonstration

Gaussian Mixture Regression (GMR) is one of the frequently used methods for trajectory learning in motion and force-based manipulation [18], [19], [20]. Tang et al. [6] use this approach to describe a probabilistic mapping from contact wrenches to twist commands for admittance control. Although using probabilistic modeling for approximating the datasets, the regression from these distributions is usually deterministic. Kronander et al. [21] use sampling from the conditional probability densities to introduce randomness in comparison to Least-Squares Estimates (LSE) and thus overcome deadlocks during assembly. Note that this is mostly valid only if the samples need not be coherent in time.

¹ All authors are with FZI Research Center for Information Technology, Haid-und-Neu-Str. 10-14, 76131 Karlsruhe, Germany {scherzinger, roennau, dillmann}@fzi.de

Al-Yacoub et al. [22] use GMR during peg-in-hole assembly tasks for clustering force-torque signals and getting insights into human-applied contact transitions and skill characteristics.

Dong et al. [23] combine a Hidden Markov Model (HMM) with Locally Weighted Regression (LWR) to learn discrete contact states of peg-in-hole assembly in a haptic simulation environment. During reproduction, they use LWR for angle corrections based on forces-torque signals in these states. Vergara et al. [24] use Probabilistic Principal Component Analysis (PPCA) for modeling kinesthetic teachings. Combining this with the constraint specifications of an optimization framework, they obtain partially transferable skills to new target positions, in which imitation learning covers wider workspace motions and constraint-based optimal control considers the last centimeters.

B. DMPs with force profiles

Dynamic Movement Primitives (DMP) [25] are an established method for encoding human-recorded motion profiles into parametric models. The inclusion of force profiles makes them suitable for contact-rich tasks, such as assembly [26]. Methods for teaching include e.g. kinesthetic guiding [27] and teleoperation [28], [29]. The latter has advantages for obtaining unbiased force profiles for not having to move the robot in its morphology. The Force profiles are often not embedded into the transformation system of the DMP, but instead are parameterized and used directly as reference setpoints in end-effector force controllers. They can be tracked in parallel to the motion trajectories, e.g. with a proportional-integral (PI) controller [26]. A compliance matrix can map the force-torque reference setpoints to motion setpoints for velocity-controlled robots. Nemeč et al. [30] and succeeding works [26], [28], [31], [29] apply this mechanism to peg-in-hole assembly tasks. Abu-Dakka et al. [26] and Savarimuthu et al. [29] further use the DMP's phase modulation to slow down the execution speed when losing track of the target force profiles in contact.

C. Our approach

Tackling force-based assembly from within offline programming requires simulation environments. Compared to using real hardware, simulation offers the advantage of supporting demonstrations with ease but usually poses high demands on realism to successfully transfer the skills to real hardware. Onda et al. [32], used a robotic manipulator as the teach device to steer objects in a frictionless simulation. Their concept did not include force feedback and purely relied on the visual channel but was sufficient to extract contact states for deriving simple position/force commands.

Applying more recent methods to this approach, we propose *sequential-probabilistic* models for encoding these complex, human strategies for low-clearance assembly, using the combination of a Mixture Density Network (MDN) [33] with Long Short-Term Memory (LSTM) [34]. For execution on real hardware, we connect this new skill model to an admittance control scheme for industrial manipulators.

III. HUMAN-INSPIRED FORCE STRATEGIES

Klingbeil et al. investigated human behavior in assembly tasks [35] and tested the hypothesis that humans ground assembly strategies in mental representations of contact states. Their results showed that some users passed a few common states during teleoperation but the intermediate behavior was mostly random among the participants. Physiological studies on control and planning through the central nervous system further showed that humans use mental *forward models* [36] to predict the response to their motor commands [37].

Concluding from these results, we propose to drop the high-level construct of contact states and model human-inspired assembly skills directly from the cyclic interaction between teleoperated force-torque commands and observed relative motion.

A. Learning features and simulation

We apply this insight to human-inspired assembly skills as follows: A user teleoperates an assembly in simulation with a joystick. In our example, the assembly consists of two plastic components, that are to be joined together with dexterity. A low clearance between the parts and complicated geometry for insertion make this a challenging benchmark, which we use to describe the concepts of this paper. Fig. 1 illustrates the overall concept. In the simulator, we record the human-initiated vector $\mathbf{f}^h \in \mathbb{R}^6$ that we apply with our fingers via the joystick to steer one of the objects. To obtain this signal, we interpret the joystick's six-axes displacement as a combined vector of forces and torques and scale that to suitable ranges for the real application. We build the simulation environment on our previous work [13], in which we describe further requirements, such as velocity-dependent damping while steering the assembly objects. Increased friction and stiction between the assembly components during demonstrations shall lead to robust strategies for the transfer to the real setup. We also record the combined position and orientation vector $\mathbf{x} \in \mathbb{R}^7$, and the goal-relative velocity $\dot{\mathbf{x}} \in \mathbb{R}^6$ during assembly. In contrast to our previous simulator, we describe both variables with respect to the estimated goal pose.

We believe that the interaction between the recorded motor commands \mathbf{f}^h and the corresponding outcome $\mathbf{x}, \dot{\mathbf{x}}$ holds concise information for learning human-inspired strategies, and the goal of this paper is to present an improved neural network controller that mimics these strategies for low-clearance assembly.

To keep equations short, we introduce two abbreviations:

$$\hat{\mathbf{x}}_t = [\mathbf{x}_t \dot{\mathbf{x}}_t \mathbf{f}_t^h]^T \quad (1)$$

$$\hat{\mathbf{y}}_t = \mathbf{f}_{t+1}^h, \quad (2)$$

in which $\hat{\mathbf{x}}_t$ is the concatenated state of all variables at the time step t and $\hat{\mathbf{y}}_t$ is the force-torque vector at the succeeding time step.

B. Data analysis

Analyzing the recorded data gives us insights into how to design the required learning algorithm. Fig. 2(a) above

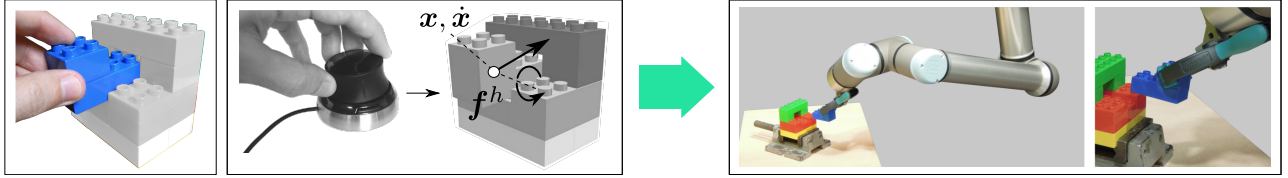


Fig. 1: From simulated teleoperation to robot-controlled execution. We use a 3Dconnexion™ 3D joystick to steer the assembly objects and solve difficult jamming situations. An LSTM-MDN model learns reactive strategies from recorded demonstrations and controls the robotic manipulator during the real assembly.

shows the z-component f_z of the motor commands \mathbf{f}^h for the exemplary assembly. This component is the vertical pushing force and is one of the characteristic variables when joining both parts at the end of the assembly. We use the Euclidean goal distance as an indicator of assembly progress. For tasks with low clearances, this distance is mostly unambiguous in geometry and provides a one-dimensional reference. The plot shows that it will not be possible to ground the force-based strategies solely in position for this assembly, because the mean loses the characteristics of the individual executions. Fig. 2(a) *below* shows the respective histogram of the z-component f_z . The darker the spots, the more frequently do these values appear in the recorded data. This also indicates in which regions it took longer to complete the assembly. Having vertical, dark areas reveals an inverse learning problem: For instance, at around 5 mm goal distance, any f_z between 0 N and -25 N seems valid, because these data appear frequently in this region in the data set. In conclusion, we need a probabilistic model to capture the non-deterministic components of f_z .

Fig. 2(b) *above* shows f_z over time for five individual recordings. The curves share patterns in specific time windows that slightly vary in scale and offset. For instance, there are characteristic pushing profiles at the end of the assembly that start at around 8 s for the fastest demonstration and at around 13 s for the slowest demonstration. While a probabilistic model could reproduce the distributions from Fig. 2(a) *below*, it could not generate predictions coherent in time as they appear in our recordings. In conclusion, we additionally need a sort of memory to model sequential patterns in the human-recorded strategies.

IV. FORCE STRATEGIES - A TEMPORAL-PROBABILISTIC APPROACH

The previous section motivated two key components in modeling force strategies for our benchmark: probabilistics to cover the multivalued character of the distributions, and memory to model their time dependencies. In this section, we describe how we include both into a temporal probabilistic model for learning force strategies for low-clearance assembly.

A. Capturing patterns in sequences

We build our model on the Long Short-Term Memory (LSTM) [38], which has been used in many domains and which excels at learning long-term dependencies in data. In contrast to feed forward networks, LSTMs maintain an

internal state, the cell state c_t , and update information via gated operations. This allows them to effectively encode long sequences of data. In our work, we use the LSTM primarily to encode time windows of past assembly progress into a concise representation and will later combine this with a probabilistic output layer to predict meaningful next force strategies with high confidence.

We combine m of these cells into an LSTM layer, allowing us to describe the forward pass with the following matrix-based equations [34], [38]:

$$\begin{aligned}
 \mathbf{f}_t &= \text{sigmoid}(\mathbf{W}_f \hat{\mathbf{x}}_t + \mathbf{b}_f + \mathbf{U}_f \mathbf{h}_{t-1}) \\
 \mathbf{i}_t &= \text{sigmoid}(\mathbf{W}_i \hat{\mathbf{x}}_t + \mathbf{b}_i + \mathbf{U}_i \mathbf{h}_{t-1}) \\
 \mathbf{o}_t &= \text{sigmoid}(\mathbf{W}_o \hat{\mathbf{x}}_t + \mathbf{b}_o + \mathbf{U}_o \mathbf{h}_{t-1}) \\
 \mathbf{c}_t &= \mathbf{f}_t \circ \mathbf{c}_{t-1} + \mathbf{i}_t \circ \tanh(\mathbf{W}_c \hat{\mathbf{x}}_t + \mathbf{b}_c + \mathbf{U}_c \mathbf{h}_{t-1}) \\
 \mathbf{h}_t &= \mathbf{o}_t \circ \tanh(\mathbf{c}_t).
 \end{aligned} \tag{3}$$

The vector $\hat{\mathbf{x}}_t \in \mathbb{R}^c$ is the input to the LSTM layer and $\mathbf{h}_t \in \mathbb{R}^m$ is the output. $\mathbf{f}_t, \mathbf{i}_t, \mathbf{o}_t \in \mathbb{R}^m$ are the activation vectors for the forget gates, the input gates, and the output gates respectively. Each has a non-recurrent weight matrix $\mathbf{W} \in \mathbb{R}^{m \times c}$ and a recurrent weight matrix $\mathbf{U} \in \mathbb{R}^{m \times m}$ for the previous hidden state $\mathbf{h}_{t-1} \in \mathbb{R}^m$. We further use \circ to denote the element-wise product. The layer-wide input \mathbf{h}_{t-1} generates recurrent connections between each cell in an LSTM layer. We use

$$\text{sigmoid}(x) = \frac{1}{1 + e^{-x}} \tag{4}$$

as activation for each element in a vector and squash inputs and outputs with the hyperbolic tangent. The weight matrices \mathbf{W}, \mathbf{b} , and \mathbf{U} include all learnable parameters. We use a single-layered LSTM and adjust the number of learnable parameters with the number of cells m in that layer.

Note that Eq. (3) yields $N + 1$ consecutive hidden states and cell states for an input sequence of consecutive points $\hat{\mathbf{x}}_{t-N}, \dots, \hat{\mathbf{x}}_t$. We are only interested in the last pair $\mathbf{h}_t, \mathbf{c}_t$, (which we refer to as the *encoding*) for which the LSTM has seen the complete input sequence:

$$\text{LSTM}(\hat{\mathbf{x}}_{t-N}, \dots, \hat{\mathbf{x}}_t) := (\mathbf{h}_t, \mathbf{c}_t) . \tag{5}$$

The next section shows how we use this encoding to estimate probabilities for the next force-torque vectors.

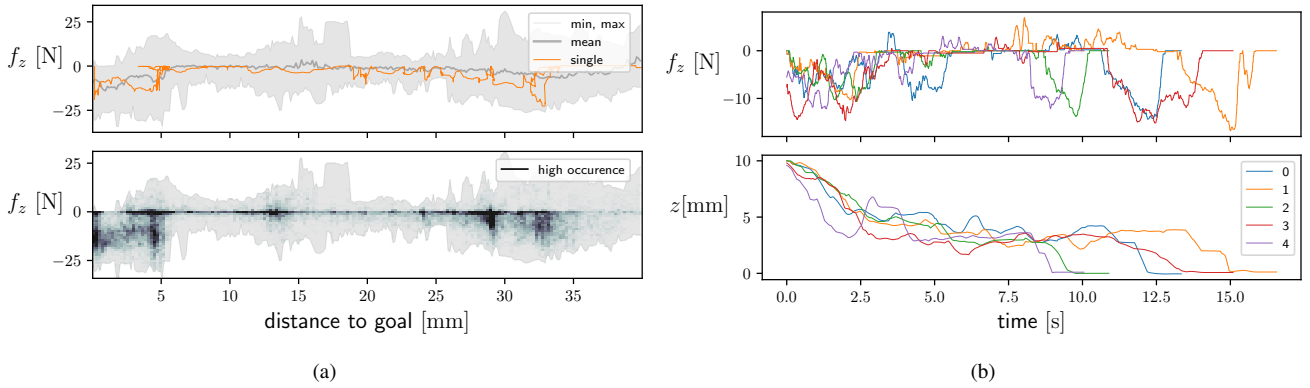


Fig. 2: Analysis of recorded demonstrations in the simulator. (a) *above* Band plot of the f_z component during 100 demonstrations. We used statistical data binning to cluster all demonstrations into vertical bins, from which we computed the min, max, and mean values, respectively. An additional, single demonstration visualizes strategies during assembly. (a) *below* The color gradient shows the qualitative occurrence of discretized values for forces f_z in a 180×60 grid. (b) *above* Time sequences for 5 performances reveal repeating patterns in f_z . (b) *below* The vertical position z shows the assembly’s progress toward zero, which indicates the end of the assembly.

B. Modeling the ambiguity in human behavior

The recorded force strategies had seemingly random trial and error, resulting in distributions for specific regions. Sampling from these distributions alone will not be successful, since those samples will not form coherent strategies over time. Using the encoding from the LSTM, however, we can model more specific distributions to sample from and thus consider past assembly progress. We use the Mixture Density Network (MDN) [33] to model these characteristics. LSTMs and MDNs have been combined for modeling highly complex human performance, such as generating human handwriting from digital text [39] or creating full-body, freestyle dance motion [40].

MDNs model conditional probability densities of the target data, conditioned on the input data [33]. In our notation, we describe this with $p(\hat{\mathbf{y}}_t | \mathbf{h}_t, \mathbf{c}_t)$, in which the hidden state \mathbf{h}_t and cell state \mathbf{c}_t are the encoding of the input sequence according to Eq. (5).

For combining the LSTM encoding and the MDN output, we feed the encoding into a fully connected layer with linear activation

$$\mathbf{z} = \mathbf{W}_z [\mathbf{h}^T, \mathbf{c}^T]^T. \quad (6)$$

The weight matrix $\mathbf{W}_z \in \mathbb{R}^{k(6+2) \times 2m}$ introduces additional learning parameters. The next step is to split \mathbf{z} into a tuple $(z^\alpha, z^\mu, z^\sigma)$ and use the individual components to parameterize a Gaussian mixture model of k Gaussian distributions $\mathcal{N}_6(\boldsymbol{\mu}, \sigma^2)$ that are each 6-dimensional. The six dimensions derive from our intention to model the 6-dimensional force-torque vector.

First, we compute normalized mixing coefficients for the Gaussians from z^α with a softmax according to

$$\alpha_i = \frac{\exp(z_i^\alpha)}{\sum_{j=1}^k \exp(z_j^\alpha)}, \quad i = 1 \dots k, \quad \alpha_i \in \mathbb{R}. \quad (7)$$

The centers of the Gaussians are computed from z^μ with

$$\boldsymbol{\mu}_i = z_{ij}^\mu, \quad i = 1 \dots k, j = 1 \dots 6, \quad \boldsymbol{\mu}_i \in \mathbb{R}^6 \quad (8)$$

and the scale parameters from z^σ with

$$\sigma_i = \exp(z_i^\sigma), \quad i = 1 \dots k, \quad \sigma_i \in \mathbb{R}. \quad (9)$$

Using these parameters, we can compute the conditional density for the i th Gaussian with [33]

$$\phi_i(\hat{\mathbf{y}}_t | \boldsymbol{\mu}_i, \sigma_i) = \frac{1}{(2\pi)^{6/2} \sigma_i^6} \exp\left(-\frac{\|\hat{\mathbf{y}}_t - \boldsymbol{\mu}_i\|^2}{2\sigma_i^2}\right). \quad (10)$$

Finally, the conditional probability density is composed of a linear combination of k Gaussian functions ϕ_i [33]

$$p(\hat{\mathbf{y}}_t | \mathbf{h}_t, \mathbf{c}_t) = \sum_{i=1}^k \alpha_i \phi_i(\hat{\mathbf{y}}_t | \mathbf{h}_t, \mathbf{c}_t). \quad (11)$$

This probability describes how likely $\hat{\mathbf{y}}_t$ follows the observed sequence $\hat{\mathbf{x}}_{t-n}, n = N \dots 0$, which we feed in form of the LSTM’s encoding $(\mathbf{h}_t, \mathbf{c}_t)$ into the MDN. The computed mixture parameters thus become functions of the encoded sequence for each time step. During training, this mechanism allows our model to solve ambiguity in the recordings by parameterizing fine-grained probability density functions along the assembly progress.

C. Data composition and training

The LSTM-MDN model is a recursive prediction model from state-action pairs to strategies. Its desired output is motor control commands \mathbf{f}^h that change the assembly object’s state $\mathbf{x}, \dot{\mathbf{x}}$, which in turn provokes a next motor command. We use supervised learning for training by splitting the recorded demonstrations in the simulator into input sequences and respective labels. Fig. 3(a) illustrates this approach. We obtain training samples from the data set by selecting individual demonstrations ξ_i out of all recorded assembly demonstrations. A pivotal time step t selects the starting point. We then compose the sample with the input sequence $\hat{\mathbf{x}}_{t-N}, \dots, \hat{\mathbf{x}}_t$ and the respective label $\hat{\mathbf{y}}_t$, which is the force-torque component of the next $\hat{\mathbf{x}}_{t+1}$.

The randomly extracted samples have an equal length of $N + 2$, so that the LSTM-MDN model has access to N

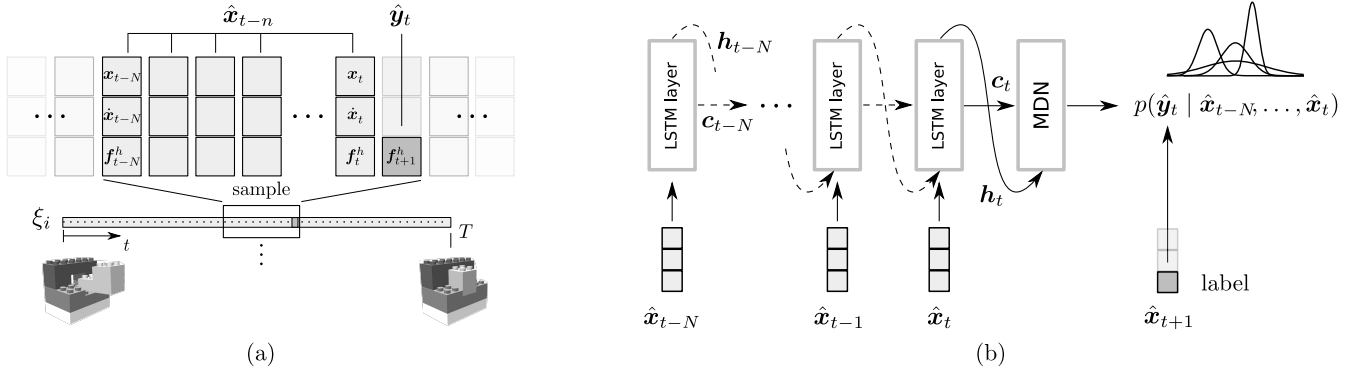


Fig. 3: (a) Composition of training samples from recorded demonstrations in simulation. (b) The unrolled LSTM-MDN model with inputs and outputs during the forward pass. The model is trained with BPTT, using the negative log-likelihood of the conditional probability density.

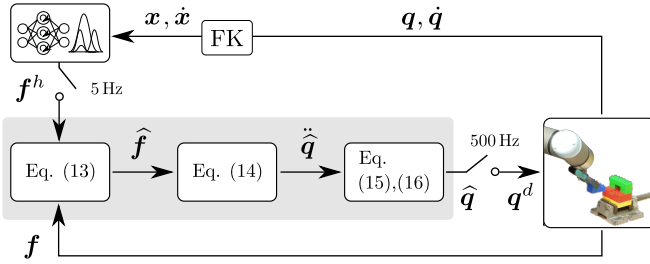


Fig. 4: Control scheme of the neural network controller for assembly. The LSTM-MDN receives state feedback from the real robot and generates force-torque references for our simulation-based force control algorithm.

time steps before predicting the corresponding probability density function. During training, we sample batches for parallel processing and cover the entirety of the training data stochastically.

We train our model with backpropagation through time (BPTT) by unrolling the model N time steps. Fig. 3(b) shows the unrolled model as a normal feedforward network. The LSTM layer's recurrent connections become normal feedforward connections and propagate the cell state and hidden state. All LSTM instances from Fig. 3(b) share a common set of learnable weights from Eq. (3) and refer to the same layer, which is illustrated at specific time steps together with the respective input from the training sequence. The fully connected output layer parameterizes the Gaussian mixture model, from which we compute the conditional probability for the given label. We finally optimize all learnable weights by minimizing the negative log-likelihood

$$\mathcal{L} = -\ln(p(\hat{y}_t | \hat{x}_{t-N}, \dots, \hat{x}_t)) \quad (12)$$

of this conditional probability density.

V. FORCE CONTROL AND ASSEMBLY SKILLS

During deployment, the LSTM-MDN model predicts 6-dimensional Gaussian distributions, from which we sample force-torque strategies for robot control in each time step. We use the forward dynamics-based control approach of our previous work [41] to realize Cartesian force control on the

robotic manipulator. Its implementation is available open-source¹. The algorithm applies the force-torque vector at the end-effector of a simulated robot and computes the corresponding joint acceleration of the system with simplified forward dynamics. The resulting motion is integrated and sent to the joint position servos of the real industrial robot. Fig. 4 shows the control scheme.

The hat symbol $\hat{(\cdot)}$ denotes *simulated* values that are computed on a simulated robot model with equal kinematics. First, we compute an error vector from the reference force-torque profile f^h as sampled from the LSTM-MDN model and the measurements f from a Cartesian force-torque sensor in contact with the environment

$$\hat{f} = K_p(f^h - f). \quad (13)$$

K_p is a positive, diagonal gain matrix. We then simulate the robot's response with

$$\hat{\ddot{q}} = \hat{H}^{-1} \hat{f}, \quad (14)$$

in which \hat{H} is a linearized joint space inertia matrix that is computed in each control cycle. We refer to our work [41] for more details on this aspect. We then obtain the joint positions \hat{q} with the Euler forward method according to

$$\hat{q}_t = \hat{q}_{t-1} + \hat{\dot{q}}_{t-1} \Delta t \quad (15)$$

$$\hat{\dot{q}}_t = \hat{\dot{q}}_{t-1} + \hat{\ddot{q}}_{t-1} \Delta t. \quad (16)$$

An additional joint damping $\hat{\dot{q}}_t \leftarrow 0.9 \hat{\dot{q}}_t$ in each simulation cycle avoids oscillations. The simulated time window Δt can be chosen independently of the robot's real control rate and allows for tweaking the controller's response to force-torque inputs. The simulated joint positions \hat{q} are then forwarded to the joint position servos of the real manipulator. Finally, we use a forward kinematics routine to compute the end-effector pose x and velocity \dot{x} , and feed them back into the LSTM-MDN model for the next prediction. Note how model inference and force control run at different rates.

¹https://github.com/fzi-forschungszentrum-informatik/cartesian_controllers

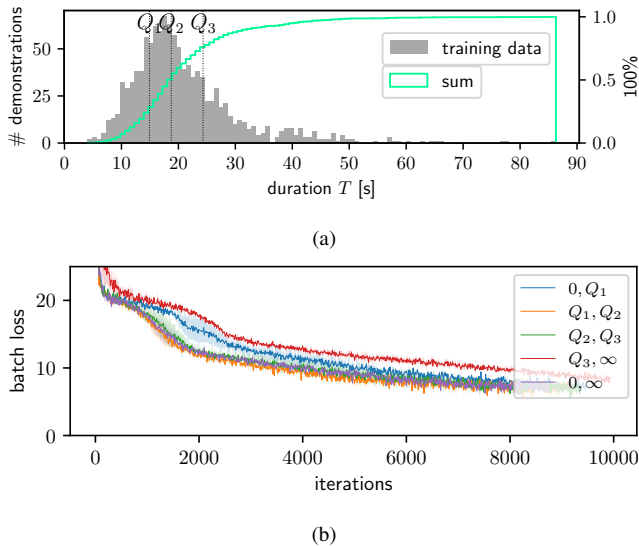


Fig. 5: (a) Histogram for the assembly benchmark consisting of 1155 demonstrations, equalling 7 hours and 10 minutes of demonstrated strategies in the simulator. The dashed lines Q_1 to Q_3 separate the datasets into equally populated quarters. (b) Learning curves of the different models, trained with $k = 4$, $N = 25$, learning rate $5 \cdot 10^{-4}$, and a minibatch size of 128.

VI. EXPERIMENTS AND RESULTS

A. Dataset and simulation

Training data usually determines the quality of data-driven models. We thus investigated how the quality of demonstrations influences the learning of assembly strategies. All demonstrations were recorded at 100 Hz from random starting poses until finishing the assembly in simulation. Since they were all successful, we use their duration as a measure of quality, implying that the shorter an assembly demonstration took, the higher the quality of the recorded strategies. We separated the training set with quartiles Q_1 - Q_3 as depicted in Fig. 5(a) and used five datasets to train on demonstrations with different duration:

- $0 \rightarrow Q_1$: up to 14.93 s
- $Q_1 \rightarrow Q_2$: between 14.93 s and 18.74 s
- $Q_2 \rightarrow Q_3$: between 18.74 s and 24.32 s
- $Q_3 \rightarrow \infty$: longer than 24.32 s
- $0 \rightarrow \infty$: all demonstrations

Fig. 5(b) shows the batch loss during training for the different models. They perform similarly in predicting the labels of the evaluation set with a slight degradation of the model trained only on the last quarter.

Continuing the experiment, we used the simulator to evaluate the different models on the assembly task. The models' predicted force-torque strategies steered the assembly object similar to as was done during demonstration with the joystick. Fig. 6 shows a successful execution. The assembly has mainly two challenging regions: The first is the insertion at 3.6 s where parts jam and tilt frequently, and the second is at 6.6 s where pressing in requires dexterity due to low-clearances. We measured success with the Euclidean distance

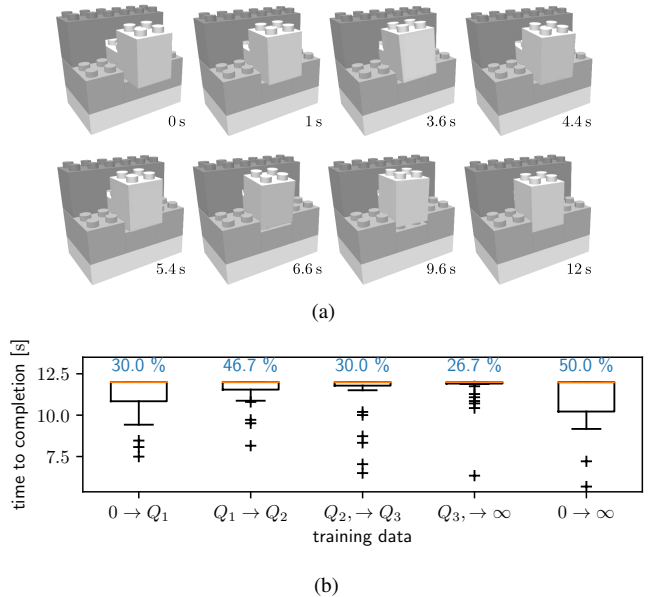


Fig. 6: (a) A successful run in simulation at 20% realtime. (b) Assembly performance in simulation with the success rate including outliers. We tested 30 trials for each model. Successful executions reached a goal distance of 0.5 mm in 12s.

to the goal pose $\|\mathbf{x}\|$ and cut off at 12s simulated time (60s realtime), after which the execution was considered a failure. Fig. 6(b) shows the results. The model trained on the complete dataset performs best on the benchmark. The model trained on the second quarter of the dataset has a similar performance, which is interesting due to using only 25% training data. This could be due to hitting a sweet spot between data quality and amount of recorded time. The model trained on the last quartile shows the lowest success rate, corresponding to the degraded learning curve from Fig. 5.

In conclusion, the quality of demonstrations in the simulator has an impact on the model to learn successful force-torque strategies and more effective (shorter) demonstrations can partially replace bigger datasets.

B. Real hardware

The goal of this experiment was to test if the strategies are portable to real-world systems through our controller. We prepared this transfer in our concept by allowing partly unrealistic mesh interpenetration in the simulator during demonstrations and increased friction and stiction between the assembly components.

Fig. 7 shows the setup. We used a passive gripper for this experiment to attach the blue assembly object to the robot's end-effector. We calibrated the setup by teleoperating the robot in force control to the goal pose of the assembly and recorded the final configuration. During execution, the model generated force-torque reference commands at 5 Hz that were executed with the force controller on the UR10e robot at 500 Hz. Fig. 8 shows the strategies and assembly progress for one such execution. During the first insertion, the parts quickly jam and require strategies to advance. Note



Fig. 7: Setup for the strategy transfer with the UR10e robot. *Left:* The assembly is clamped in a vice and glued to a surface with adhesive tape. *Right:* The blue object is glued to the jaws of a non-actuated gripper, whose elasticity adds uncertainty to the system.

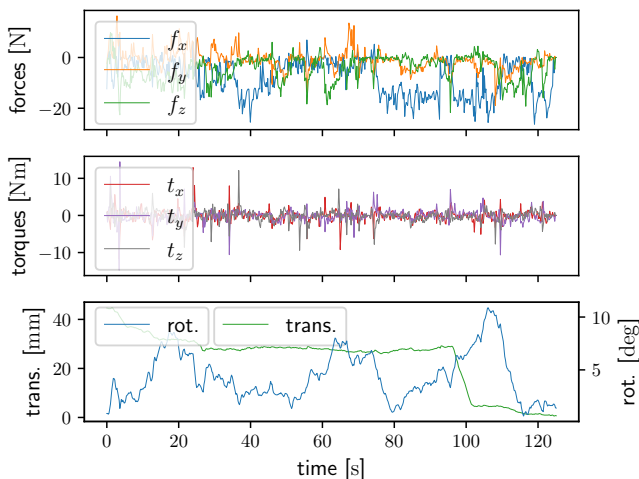


Fig. 8: Commanded force-torque strategies for a successful assembly on the real setup.

how the model makes several forward push attempts with the swings of the f_x component. Since this is not immediately successful, the model tries different re-orientations while searching for part clearance. After approximately 95s, the strategies are successful and finally plug both parts together. The execution is shown in full length in the accompanying video.

VII. DISCUSSION

During the executions on the real setup, configurations that significantly differed from the dataset decreased the model’s performance. Real-world assemblies might have several local optima along the goal where parts can be put in unseen and wrong configurations, leading to possible deadlocks. If these spots are known or can be anticipated, they should be included randomly as challenges in the simulator to increase the model’s robustness.

A further limitation is the speed of execution. Admittance controlled industrial robots that close force control around position-controlled joints, are not stable during interaction with stiff environments at human speed. It might thus be worthwhile to deploy this model together with an impedance-controlled robot.

When programming an assembly with our approach, some experience with the real parts is required to set suitable ranges for the force-torque signals and to apply meaningful strategies in the simulator. It is also helpful to touch the real

assembly parts to better imagine how they combine in the simulator. The strength of our approach is, however, that the predicted strategies can be post-scaled and sanity-checked before sending them to the controller. For instance, the force-torque strategies’ amplitude could be decreased by 50% on the first run.

VIII. CONCLUSIONS

In this work, we proposed a method to learn human-inspired assembly strategies from simulated teleoperation. We addressed two challenges that are common in Imitation Learning for force-sensitive assembly tasks: Handling low clearances with tight-fitting parts that require much trial and error, and learning these strategies offline without access to the real hardware. Basing our ideas on data analysis of recorded demonstrations, we combined an LSTM-based encoder with an MDN to model probabilistic force strategies that follow patterns over time. We evaluated this approach experimentally in simulation and on real hardware with an exemplary benchmark. The results showed that human-inspired strategies that are learned from simulated data with our method are concise enough to be successfully transferred to a real robot.

In future research, we plan to reduce the sample intensity that is currently required in the simulator. A promising method could be including Offline RL [42] on the demonstration data to exceed human performance without further interaction with the simulator.

REFERENCES

- [1] Zengxi Pan et al. “Recent progress on programming methods for industrial robots”. In: *Robotics and Computer-Integrated Manufacturing* 28.2 (2012), pp. 87–94.
- [2] S. Gottschlich, C. Ramos, and D. Lyons. “Assembly and task planning: a taxonomy”. In: *IEEE Robotics Automation Magazine* 1.3 (1994), pp. 4–12.
- [3] W.S. Newman et al. “Force-responsive robotic assembly of transmission components”. In: *Robotics and Automation, 1999. Proceedings. 1999 IEEE International Conference on*. Vol. 3. 1999, 2096–2102 vol.3.
- [4] In-Wook Kim, Dong-Jin Lim, and Kab-Il Kim. “Active peg-in-hole of chamferless parts using force/moment sensor”. In: *Proceedings 1999 IEEE/RSJ International Conference on Intelligent Robots and Systems. Human and Environment Friendly Robots with High Intelligence and Emotional Quotients (Cat. No.99CH36289)*. Vol. 2. Oct. 1999, 948–953 vol.2.
- [5] Wyatt S Newman, Yonghong Zhao, and Y-H Pao. “Interpretation of force and moment signals for compliant peg-in-hole assembly”. In: *Proceedings 2001 ICRA. IEEE International Conference on Robotics and Automation (Cat. No. 01CH37164)*. Vol. 1. IEEE, 2001, pp. 571–576.
- [6] Te Tang et al. “Autonomous alignment of peg and hole by force/torque measurement for robotic assembly”. In: *2016 IEEE international conference on automation science and engineering (CASE)*. IEEE, 2016, pp. 162–167.
- [7] A. Wahrburg et al. “Combined pose-wrench and state machine representation for modeling Robotic Assembly Skills”. In: *IEEE/RSJ International Conference on Intelligent Robots and Systems (IROS)*. 2015, pp. 852–857.

- [8] A. Stemmer, A. Albu-Schaffer, and G. Hirzinger. “An Analytical Method for the Planning of Robust Assembly Tasks of Complex Shaped Planar Parts”. In: *Robotics and Automation, 2007 IEEE International Conference on*. Apr. 2007, pp. 317–323.
- [9] L. Johannsmeier, M. Gerchow, and S. Haddadin. “A Framework for Robot Manipulation: Skill Formalism, Meta Learning and Adaptive Control”. In: *2019 International Conference on Robotics and Automation (ICRA)*. May 2019, pp. 5844–5850.
- [10] Sergey Levine et al. “End-to-end training of deep visuomotor policies”. In: *arXiv preprint arXiv:1504.00702* (2015).
- [11] Tadanobu Inoue et al. “Deep reinforcement learning for high precision assembly tasks”. In: *arXiv preprint arXiv:1708.04033* (2017).
- [12] Gerrit Schoettler et al. “Deep Reinforcement Learning for Industrial Insertion Tasks with Visual Inputs and Natural Rewards”. In: *arXiv preprint arXiv:1906.05841* (2019).
- [13] S. Scherzinger, A. Roennau, and R. Dillmann. “Contact Skill Imitation Learning for Robot-Independent Assembly Programming”. In: *IEEE/RSJ International Conference on Intelligent Robots and Systems (IROS)*. Nov. 2019, pp. 4309–4316.
- [14] Rüdiger Dillmann, M Kaiser, and Ales Ude. “Acquisition of elementary robot skills from human demonstration”. In: *International Symposium on Intelligent Robotics Systems*. Citeseer. 1995, pp. 185–192.
- [15] Aude Billard et al. “Robot programming by demonstration”. In: *Springer handbook of robotics*. Springer, 2008, pp. 1371–1394.
- [16] Stefan Schaal. “Is imitation learning the route to humanoid robots?” In: *Trends in cognitive sciences* 3.6 (1999), pp. 233–242.
- [17] Michael Bain and Claude Sammut. “A Framework for Behavioural Cloning.” In: *Machine Intelligence 15*. 1995, pp. 103–129.
- [18] Micha Hersch et al. “Dynamical system modulation for robot learning via kinesthetic demonstrations”. In: *IEEE Transactions on Robotics* 24.6 (2008), pp. 1463–1467.
- [19] S. Calinon et al. “Handling of multiple constraints and motion alternatives in a robot programming by demonstration framework”. In: *2009 9th IEEE-RAS International Conference on Humanoid Robots*. 2009, pp. 582–588.
- [20] L. Rozo et al. “Learning Physical Collaborative Robot Behaviors From Human Demonstrations”. In: *IEEE Transactions on Robotics* 32.3 (2016), pp. 513–527.
- [21] Klas Kronander, Etienne Burdet, and Aude Billard. “Task transfer via collaborative manipulation for insertion assembly”. In: *Workshop on human-robot interaction for industrial manufacturing, robotics, science and systems*. Citeseer. 2014.
- [22] Ali Al-Yacoub et al. “Symbolic-based recognition of contact states for learning assembly skills”. In: *Frontiers in Robotics and AI* 6 (2019), p. 99.
- [23] Shen Dong and Fazel Naghdy. “Application of hidden Markov model to acquisition of manipulation skills from haptic rendered virtual environment”. In: *Robotics and Computer-Integrated Manufacturing* 23.3 (2007), pp. 351–360.
- [24] C. A. Vergara P., J. De Schutter, and E. Aertbeliën. “Combining Imitation Learning With Constraint-Based Task Specification and Control”. In: *IEEE Robotics and Automation Letters* 4.2 (Apr. 2019), pp. 1892–1899.
- [25] Auke Jan Ijspeert et al. “Dynamical movement primitives: learning attractor models for motor behaviors”. In: *Neural computation* 25.2 (2013), pp. 328–373.
- [26] Fares J Abu-Dakka et al. “Adaptation of manipulation skills in physical contact with the environment to reference force profiles”. In: *Autonomous Robots* 39.2 (2015), pp. 199–217.
- [27] Aljaž Kramberger et al. “Transfer of contact skills to new environmental conditions”. In: *IEEE*. 2016, pp. 668–675.
- [28] Norbert Krüger et al. “Technologies for the Fast Set-Up of Automated Assembly Processes”. In: *KI-Künstliche Intelligenz* 28.4 (2014), pp. 305–313.
- [29] T. R. Savarimuthu et al. “Teaching a Robot the Semantics of Assembly Tasks”. In: *IEEE Transactions on Systems, Man, and Cybernetics: Systems* PP.99 (2017), pp. 1–23.
- [30] B. Nemeč et al. “Transfer of assembly operations to new workpiece poses by adaptation to the desired force profile”. In: *16th International Conference on Advanced Robotics (ICAR)*. Nov. 2013, pp. 1–7.
- [31] Aljaz Kramberger et al. “Generalization of orientation trajectories and force-torque profiles for robotic assembly”. In: *Robotics and Autonomous Systems* 98 (2017), pp. 333–346.
- [32] H. Onda, H. Hirukawa, and K. Takase. “Assembly motion teaching system using position/force simulator - extracting a sequence of contact state transition”. In: *IEEE/RSJ International Conference on Intelligent Robots and Systems (IROS)*. 1995, pp. 9–16.
- [33] Christopher M Bishop. *Mixture density networks*. Tech. rep. Citeseer, 1994.
- [34] Sepp Hochreiter and Jürgen Schmidhuber. “Long short-term memory”. In: *Neural computation* 9.8 (1997), pp. 1735–1780.
- [35] Ellen Klingbeil, Samir Menon, and Oussama Khatib. “Experimental Analysis of Human Control Strategies in Contact Manipulation Tasks”. In: *2016 International Symposium on Experimental Robotics*. Ed. by Dana Kulić et al. Cham: Springer International Publishing, 2017, pp. 275–286.
- [36] Michael I Jordan and Robert A Jacobs. “Hierarchies of adaptive experts”. In: *Advances in neural information processing systems*. 1992, pp. 985–992.
- [37] R.C. Miall and D.M. Wolpert. “Forward Models for Physiological Motor Control”. In: *Neural Networks* 9.8 (1996). Four Major Hypotheses in Neuroscience, pp. 1265–1279.
- [38] Felix A. Gers, Jürgen Schmidhuber, and Fred A. Cummins. “Learning to Forget: Continual Prediction with LSTM”. In: *Neural Computation* 12 (2000), pp. 2451–2471.
- [39] Alex Graves. “Generating sequences with recurrent neural networks”. In: *arXiv preprint arXiv:1308.0850* (2013).
- [40] Luka Crnkovic-Friis and Louise Crnkovic-Friis. “Generative choreography using deep learning”. In: *arXiv preprint arXiv:1605.06921* (2016).
- [41] Stefan Scherzinger, Arne Roennau, and Rüdiger Dillmann. *Virtual Forward Dynamics Models for Cartesian Robot Control*. 2020. arXiv: 2009.11888 [cs, RO].
- [42] Ilya Kostrikov, Ashvin Nair, and Sergey Levine. *Offline Reinforcement Learning with Implicit Q-Learning*. 2021.